

Metabolic independence drives gut microbial colonization and resilience in health and disease

Andrea R. Watson^{1,2,‡}, Jessika Füssel^{1,3,‡}, Iva Veseli^{4,‡}, Johanna Zaal DeLongchamp⁵, Marisela Silva⁵, Florian Trigodet¹, Karen Lolans¹, Alon Shaiber⁴, Emily Fogarty^{1,2}, Joseph M. Runde⁶, Christopher Quince⁷, Michael K. Yu⁸, Arda Söylev⁹, Hilary G. Morrison¹⁰, Sonny T.M. Lee¹, Dina Kao¹¹, David T. Rubin¹, Bana Jabri¹, Thomas Louie⁵, A. Murat Eren^{1,2,3,10,12,*}

¹Department of Medicine, The University of Chicago, Chicago, IL 60637, USA

²Committee on Microbiology, The University of Chicago, Chicago, IL 60637, USA

³Institute for Chemistry and Biology of the Marine Environment, University of Oldenburg, 26129 Oldenburg, Germany

⁴Biophysical Sciences Program, The University of Chicago, Chicago, IL 60637, USA

⁵Department of Medicine, The University of Calgary, Calgary, AB T2N 1N4, Canada

⁶Department of Pediatrics, Lurie Children's Hospital of Chicago, Chicago, IL 60611, USA

⁷Organisms and Ecosystems, Earlham Institute, Norwich, Norwich, NR4 7UZ, United Kingdom

⁸Toyota Technological Institute at Chicago, Chicago, IL 60637, USA

⁹Department of Computer Engineering, Konya Food and Agriculture University, Konya, Turkey

¹⁰Josephine Bay Paul Center, Marine Biological Laboratory, Woods Hole, MA 02543, USA

¹¹Department of Medicine, University of Alberta, Edmonton, AB T6G 2G3, Canada

¹²Helmholtz Institute for Functional Marine Biodiversity, 26129 Oldenburg, Germany

* Corresponding author: meren@hifmb.de

‡ These authors contributed equally

Running Title Drivers of human gut colonization

Keywords fecal microbiota transplantation; human gut microbiome; microbial colonization; microbial metabolism; metabolic independence

Abstract

Changes in microbial community composition as a function of human health and disease states have sparked remarkable interest in the human gut microbiome. However, establishing reproducible insights into the determinants of microbial succession in disease has been a formidable challenge. Here we use fecal microbiota transplantation (FMT) as an *in natura* experimental model to investigate the association between metabolic independence and resilience in stressed gut environments. Our genome-resolved metagenomics survey suggests that FMT serves as an environmental filter that favors populations with higher metabolic independence, the genomes of which encode complete metabolic modules to synthesize critical metabolites, including amino acids, nucleotides, and vitamins. Interestingly, we observe higher completion of the same biosynthetic pathways in microbes enriched in IBD patients. These observations suggest a general mechanism that underlies changes in diversity in perturbed gut environments, and reveal taxon-independent markers of ‘dysbiosis’ that may explain why widespread yet typically low abundance members of healthy gut microbiomes can dominate under inflammatory conditions without any causal association with disease.

Introduction

Understanding the determinants of microbial colonization is one of the fundamental aims of gut microbial ecology (Costello et al. 2012; Messer et al. 2017). The gradual maturation of the microbiome during the first months of life (Stewart et al. 2018), the importance of diet and lifestyle in shaping the gut microbiome (Koenig et al. 2011; Rothschild et al. 2018), and the biogeography of microbial populations along the gastrointestinal tract (Donaldson, Lee, and Mazmanian 2016) strongly suggest the importance of niche-based interactions between the gut environment and its microbiota. Previous studies that described such interactions in the context of microbial colonization have focused on microbial succession in infant gut microbiomes (Stewart et al. 2018), or relied on model systems such as germ free mice conventionalized with a consortium of microbial isolates

from infant stool (Feng et al. 2020). However, our understanding of the ecological underpinnings of secondary succession following a major ecosystem disturbance caused by complex environmental factors in the gut microbiome remains incomplete. A wide range of diseases and disorders are associated with such disturbances, (Almeida et al., 2020; Durack and Lynch, 2019; Lynch and Pedersen, 2016), however; mechanistic underpinnings of these associations have been difficult to resolve. This is in part due to the diversity of human lifestyles (David et al., 2014), and the limited utility of model systems to make robust causal inferences for microbially mediated human diseases (Walter et al., 2020).

Inflammatory bowel disease (IBD), a group of increasingly common intestinal disorders that cause inflammation of the gastrointestinal tract (Baumgart and Carding 2007), has been a model to study human diseases associated with the gut microbiota (Schirmer et al. 2019). The pathogenesis of IBD is attributed in part to the gut microbiome (Plichta et al. 2019), yet the microbial ecology of IBD-associated dysbiosis remains a puzzle. Despite marked changes in gut microbial community composition in IBD (Ott et al. 2004; Sokol and Seksik 2010; Joossens et al. 2011), the microbiota associated with the disease lacks acquired infectious pathogens (Chow, Tang, and Mazmanian 2011), and microbes that are found in IBD typically also occur in healthy individuals (Clooney et al. 2021), which complicates the search for robust functional or taxonomic markers of health and disease states (Lloyd-Price et al. 2019). One of the hallmarks of IBD is reduced microbial diversity during episodes of inflammation, when the gut environment is often dominated by microbes that typically occur in lower abundances prior to inflammation (Vineis et al. 2016). The sudden increase in the relative abundance of microbes that are also common to healthy individuals suggests that the harsh conditions of IBD likely act as an ecological filter that eliminates some populations while allowing others to bloom. Yet, in the absence of an understanding of the genetic requirements for survival in IBD, critical insights into the functional drivers of microbial community succession in such disease states remains elusive.

Fecal microbiota transplantation (FMT), the transfer of stool from a donor into a recipient's gastrointestinal tract (Eiseman et al. 1958), represents an experimental middleground to

capture complex ecological interactions that shape the microbial community during secondary succession of a disrupted gut environment. FMT is frequently employed in the treatment of recurrent *Clostridioides difficile* infection (CDI) (van Nood et al. 2013) that can cause severe diarrhea and intestinal inflammation. In addition to its medical utility, FMT offers a powerful framework to study fundamental questions of microbial ecology by colliding the microbiome of a healthy donor with the disrupted gut environment of the recipient. The process presents an ecological filter with the potential to reveal functional determinants of microbial colonization success and resilience in impaired gut environments (Schmidt, Raes, and Bork 2018).

Here we use FMT as an *in natura* experimental model to investigate the ecological and functional determinants of successful colonization of the human gut at the level of individual microbial populations using genome-resolved metagenomics. Our findings highlight the importance of environmental selection acting on the biosynthetic capacity for essential nutrients as a key driver of colonization outcome after FMT and resilience during inflammation, and demonstrate that metabolic independence serves as a taxonomy-independent determinant of colonization success in the human gut.

Results and Discussion

Study Design

Our study includes 109 gut metagenomes (Supplementary Table 1) from two healthy FMT donors (A and B) and 10 FMT recipients (five recipients per donor) with multiple recurrent CDI. We collected 24 Donor A samples over a period of 636 days and 15 Donor B samples over a period of 532 days to establish an understanding of the long-term microbial population dynamics within each donor microbiota. The FMT recipients received vancomycin for a minimum of 10 days to attain resolution of diarrheal illness prior to FMT. On the last day of vancomycin treatment, a baseline fecal sample was collected from each recipient, and their bowel contents were evacuated immediately prior to FMT. Recipients did not take any antibiotics on the day of transplant, or during the post-FMT sampling period (Supplementary Figure 1). We collected 5 to 9 samples from each

recipient for a period of up to 336 days post-FMT. Deep sequencing of donor and recipient metagenomes using Illumina paired-end (2x150) technology resulted in a total of 7.7 billion sequences with an average of 71 million reads per metagenome (Figure 1, Supplementary Table 1, Supplementary Table 2). We employed genome-resolved metagenomics, microbial population genetics, and metabolic pathway reconstruction for an in-depth characterization of donor and recipient gut microbiotas, and we leveraged publicly available gut metagenomes to benchmark our observations.

Genome-resolved metagenomics show many, but not all, donor microbes colonized recipients and persisted long-term

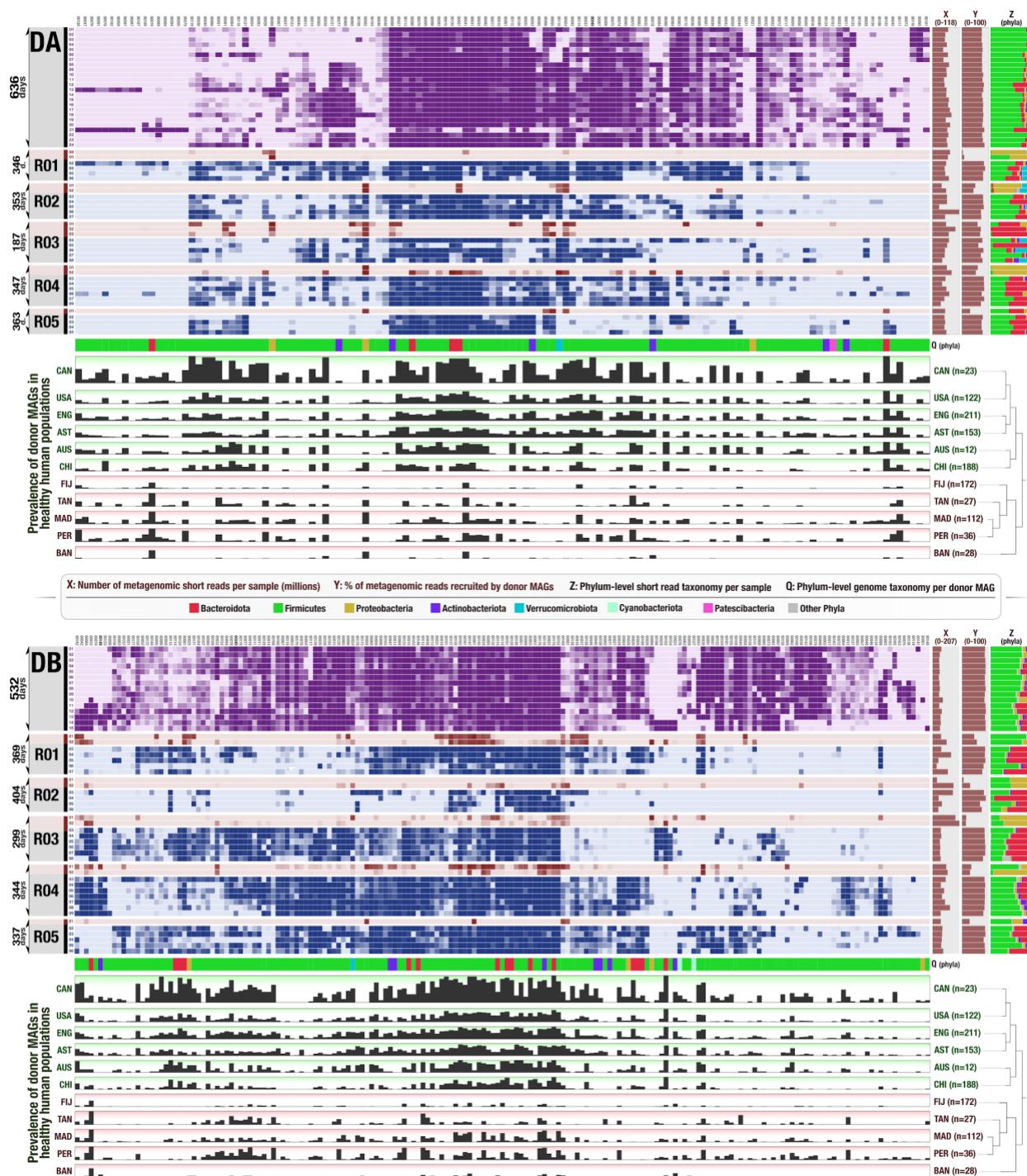
We first characterized the taxonomic composition of each donor and recipient sample by analyzing our metagenomic short reads given a clade-specific k-mer database (Supplementary Table 2). The phylum-level microbial community composition of both donors reflected those observed in healthy individuals in North America (Human Microbiome Project Consortium 2012): a large representation of Firmicutes and Bacteroidetes, and other taxa with lower relative abundances including Actinobacteria, Verrucomicrobia, and Proteobacteria (Figure 1, Supplementary Table 2). In contrast, the vast majority of the recipient pre-FMT samples were dominated by Proteobacteria, a phylum that typically undergoes a drastic expansion in individuals treated with vancomycin (Isaac et al. 2017). After FMT, we observed a dramatic shift in recipient taxonomic profiles (Supplementary Table 2, Supplementary Figure 2, Supplementary Figure 3), a widely documented hallmark of this procedure (Khoruts et al. 2010; Grehan et al. 2010; Shahinas et al. 2012). Nearly all recipient samples post-FMT were dominated by Bacteroidetes and Firmicutes as well as Actinobacteria and Verrucomicrobia in lower abundances, resembling qualitatively, but not quantitatively, the taxonomic profiles of their donors (Supplementary Table 2). The phylum Bacteroidetes was over-represented in recipients: even though the median relative abundance of Bacteroidetes populations were 5% and 17% in donors A and B, their relative abundance in recipients post-FMT was 33% and 45%, respectively (Figure 1, Supplementary Table 2). A single genus, *Bacteroides*, made up 76% and 82% of the Bacteroidetes populations in the recipients of

115 Donor A and B, respectively (Supplementary Table 2). The success of the donor
Bacteroides populations in recipients upon FMT is not surprising given the ubiquity of this
genus across geographically diverse human populations (Wexler and Goodman 2017)
and the ability of its members to survive substantial levels of stress (Swidsinski et al.
2005; Vineis et al. 2016). This initial coarse taxonomic analysis demonstrates the
120 successful transfer of only some populations, suggesting selective filtering of the
transferred community.

To generate insights into the genomic content of the microbial community, we first
assembled short metagenomic reads into contiguous segments of DNA (contigs). Co-
assemblies of 24 Donor A and 15 Donor B metagenomes independently resulted in
125 53,891 and 54,311 contigs that were longer than 2,500 nucleotides and described 0.70
and 0.79 million genes occurring in 179 and 248 genomes, as estimated by the mode of
the frequency of bacterial single-copy core genes (Supplementary Table 2). On average,
80.8% of the reads in donor metagenomes mapped back to the assembled contigs from
donor metagenomes, which suggests that the assemblies represented a large fraction of
130 the donor microbial communities. Donor assemblies recruited only 43.4% of the reads on
average from the pre-FMT recipient metagenomes. This number increased to 80.2% for
post-FMT recipient metagenomes and remained at an average of 76.8% even one year
post-FMT (Supplementary Table 2). These results suggest that members of the donor
microbiota successfully established in the recipient gut and persisted long-term.

135 To investigate functional determinants of microbial colonization by identifying donor
populations that were successful at colonizing multiple individuals, we reconstructed
microbial genomes from donor assemblies using sequence composition and differential
coverage signal as previously described (Sharon et al. 2013; Lee et al. 2017). We
manually refined metagenomic bins to improve their quality following previously described
140 approaches (Delmont et al. 2018; Shaiber et al. 2020) and only retained those that were
at least 70% complete and had no more than 10% redundancy as predicted by bacterial
single-copy core genes (Bowers et al. 2017; Chen et al. 2020). Our binning effort resulted
in a final list of 128 metagenome-assembled genomes (MAGs) for Donor A and 183
MAGs for Donor B that included members of Firmicutes (n=265), Bacteroidetes (n=20),

145 Actinobacteria (n=14), Proteobacteria (n=7), Verrucomicrobia (n=2), Cyanobacteria
(n=2), and Patescibacteria (n=1) (Supplementary Table 3). The taxonomy of donor-
derived genomes largely reflected the taxonomic composition of donor metagenomic
short reads (Figure 1, Supplementary Table 2, Supplementary Table 3). While only 20
150 Bacteroidetes group, we recovered 265 genomes that represented lower abundance but
diverse populations of Firmicutes (Figure 1, Supplementary Table 2, Supplementary
Table 3).



155 **Figure 1. Detection of FMT donor genomes in FMT recipients and publicly available gut metagenomes.** In both heat maps each column represents a donor genome, each row represents a metagenome, and each data point represents the detection of a given genome in a given metagenome. Genomes are clustered according to their detection in all metagenomes (Euclidean distance and Ward clustering). Purple rows represent donor metagenomes from stool samples collected over 636 days for Donor A and 532 days for Donor B. Red rows represent recipient pre-FMT metagenomes, and blue rows represent recipient post-FMT metagenomes. The three rightmost columns display for

160 each metagenome: (X) the number of metagenomic short reads in millions, (Y) the percent of metagenomic short reads
recruited by genomes, and (Z) the taxonomic composition of metagenomes (based on metagenomic short reads) at
the phylum level. The first row below each heat map (Q) provides the phylum-level taxonomy for each donor genome.
Finally, the 11 bottommost rows under each heat map show the fraction of healthy adult metagenomes from 11 different
165 countries in which a given donor genome is detected (if a genome is detected in every individual from a country it is
represented with a full bar). The dendrograms on the right-hand side of these layers organize countries based on the
detection patterns of genomes (Euclidean distance and Ward clustering). Red and green shades represent the two
main clusters that emerge from this analysis, where green layers are industrialized countries in which donor genomes
are highly prevalent and red layers are less industrialized countries where the prevalence of donor genomes is low. A
high resolution version of this figure is also available at <https://doi.org/10.6084/m9.figshare.15138720>.

170 Metagenomic read recruitment elucidates colonization events

Reconstructing donor genomes enabled us to characterize (1) population-level microbial
colonization dynamics before and after FMT using donor and recipient metagenomes and
(2) the distribution of each donor population across geographically distributed humans
using 1,984 publicly available human gut metagenomes (Figure 1, Supplementary Table
175 4).

Our metagenomic read recruitment analysis showed that donor A and B genomes
recruited on average 77.05% and 83.04%, respectively, of reads from post-FMT
metagenomes, suggesting that the collection of donor genomes well represents the
recipient metagenomes post-FMT (Figure 1). As expected, we detected each donor
180 population in at least one donor metagenome (see Methods for 'detection' criteria). Yet,
only 16% of Donor A populations were detected in every Donor A sample, and only 44%
of Donor B populations were detected in every Donor B sample (Figure 1, Supplementary
Table 3), demonstrating the previously documented dynamism of gut microbial
community composition over time (David et al. 2014). A marked increase in the detection
185 of donor populations in recipients after FMT is in agreement with the general pattern of
transfer suggested by the short-read taxonomy (Figure 1): while we detected only 38% of
Donor A and 54% of Donor B populations in at least one recipient pre-FMT, these
percentages increased to 96% for both donors post-FMT (Supplementary Table 3). We
note that we observed a higher fraction of donor populations in recipients as a function of
190 the FMT delivery method. Following the cases of FMT where donor stool was
transplanted via colonoscopy, we detected 54.7% and 33.3% donor genomes in the

recipients of donor A (n=3) and donor B (n=2), respectively. In contrast, in the cases of FMT where donor stool was transplanted via pills, we detected 69.5% and 61.6% donor genomes in the recipients of donor A (n=2) and donor B (n=3), respectively.

195 Not every donor population was detected in each recipient, but the emergence of donor populations in recipients did not appear to be random: while some donor populations colonized all recipients, others colonized none (Figure 1), providing us with an opportunity to quantify colonization success for each donor population in our dataset.

200 Succession of donor microbial populations in FMT recipients and their prevalence in publicly available metagenomes reveal good and poor colonizers

Of the populations that consistently occurred in donor metagenomes, some were absent in all or most recipient metagenomes after FMT, and others were continuously present throughout the sampling period in both donor and recipient metagenomes (Figure 1). To
205 gain insights into the ecology of donor microbial populations beyond our dataset, we explored their occurrence in publicly available healthy gut metagenomes through metagenomic read recruitment. This analysis enabled us to consider the prevalence of donor populations in FMT recipients and global gut metagenomes and to define two
210 groups of donor genomes that represented opposite colonization and prevalence phenotypes.

The 'good colonizers' comprise those microbial populations that colonized and persisted in all FMT recipients. Intriguingly, these populations were also the most prevalent in publicly available gut metagenomes from Canada. Overall, these donor microbial
215 populations (1) systematically colonized the majority of FMT recipients, (2) persisted in these environments long-term regardless of host genetics or lifestyle, and (3) were prevalent in public gut metagenomes outside of our study. In contrast, the so-called 'poor colonizers' failed to colonize or persist in at least three FMT recipients. These populations were nevertheless viable in the donor gut environment: not only did they occur

220 systematically in donor metagenomes, but they also sporadically colonized some FMT recipients. Yet, unlike the good colonizers, the distribution patterns of poor colonizers were sparse within our cohort, as well as within the publicly available metagenomes. In fact, populations identified as poor colonizers were less prevalent than good colonizers in each of the 17 different countries we queried. In countries including the United States, 225 Canada, Austria, China, England, and Australia, microbial populations identified as good colonizers occurred in 5 times more people than poor colonizers in the same country (Figure 1, Supplementary Table 3), which suggests that the outcomes of FMT in our dataset were unlikely determined by neutral processes. This observation is in contrast with previous studies that suggested ‘dose’ (i.e., the abundance of a given population in 230 donor fecal matter) as a predominant force that determines outcomes of colonization after FMT (Podlesny and Florian Fricke, 2020; Smillie et al., 2018). However, our strain-resolved analysis of colonization events in our data in conjunction with the distribution of the same populations in publicly available metagenomes revealed (1) a significant correlation between the colonization success of donor populations and their prevalence 235 across publicly available metagenomes, and (2) showed that the prevalence of a given population across global gut metagenomes can predict its colonization success after FMT better than its abundance in the donor stool sample (Wald test, $p=6.3e-06$ and $p=9.0e-07$) (Supplementary Information). Overall, these observations suggest a link between the colonization outcomes in our study and global prevalence of the same microbial 240 populations, and that the succession of donor populations in our data were likely influenced by selective processes that influence colonization outcomes.

Next, we sought to investigate whether we can identify metabolic features that systematically differ between good colonizers and poor colonizers independent of their taxonomy. To conduct such a comparative analysis, we conservatively selected the top 245 20 populations from each group that best reflect their group properties by considering both their success after FMT and their prevalence across publicly available metagenomes (Supplementary Table 7). The 20 populations representative of good colonizers were dominated by Firmicutes (15 of 20) but also included Bacteroidetes and one Actinobacteria population. All populations identified as poor colonizers resolved to 250 Firmicutes (Figure 2, Supplementary Table 7). Genome completion estimates did not

differ between good and poor colonizers (Wilcoxon rank sum test, $p=0.42$) and averaged to 91% and 93%, respectively. But intriguingly, the genome sizes between the two groups differed dramatically ($p=2.9e-06$): genomes of good colonizers averaged to 2.8 Mbp while those of poor colonizers averaged to 1.6 Mbp. We considered that our bioinformatics analyses may have introduced biases to genome lengths, but found a very high correspondence between the lengths of the genomes and their best matching reference genomes in the Genome Taxonomy Database (GTDB) ($R^2=0.88$, $p=5e-14$). Assuming that the generally larger genomes of good colonizers may be an indication of an increased repertoire of core metabolic competencies compared to poor colonizers, we next conducted a metabolic enrichment analysis for quantitative insights (see Materials and Methods).

Good colonizers are enriched in metabolic pathways for the biosynthesis of essential organic compounds

Our enrichment analysis between good and poor colonizers revealed 33 metabolic modules that were enriched in good colonizers and none that were enriched in poor colonizers (Figure 2, Supplementary Table 7). Of all enriched modules, 79% were related to biosynthesis, indicating an overrepresentation of biosynthetic capabilities among good colonizers as KEGG modules for biosynthesis only make up 55% of all KEGG modules (Figure 2, Supplementary Table 7). Of the 33 enriched modules, 48.5% were associated with amino acid metabolism, 21.2% with vitamin and cofactor metabolism, 18.2% with carbohydrate metabolism, 24.2% with nucleotide metabolism, 6% with lipid metabolism and 3% with energy metabolism (Supplementary Table 7). Metabolic modules that were enriched in the good colonizers included the biosynthesis of seven of nine essential amino acids, indicating the importance of high metabolic independence to synthesize essential compounds as a likely factor that increases success in colonizing new environments (Supplementary Table 7). This is further supported by the enrichment of biosynthesis pathways for the essential cofactor vitamin B12 (cobalamin), which occurred in 67.5% of the good colonizers and only 12.5% of the poor colonizers (Supplementary Table 7). Vitamin B12 is structurally highly complex and costly to produce, requiring expression of

280 more than 30 genes that are exclusively encoded by bacteria and archaea (J. H. Martens
et al. 2002). In addition to the biosynthesis of tetrahydrofolate, riboflavin, and cobalamin,
the genomes of good colonizers had a larger representation of biosynthetic modules for
vitamins including biotin, pantothenate, folate, and thiamine (Supplementary Table 7).
These micronutrients are equally essential in bacterial and human metabolism and are
285 important mediators of host-microbe interactions (Biesalski 2016). Interestingly, enriched
metabolic modules in our analysis partially overlap with those that Feng *et al.* identified
as the determinants of microbial fitness using metatranscriptomics and a germ-free
mouse model conventionalized with microbial isolates of human origin (Feng et al. 2020).

Even though these 33 metabolic modules were statistically enriched in populations
290 identified as good colonizers, some of them also occurred in the genomes of poor
colonizers (Figure 2). To identify whether the levels of completion of these modules could
distinguish the good and poor colonizers, we matched six good colonizers that encoded
modules enriched in these populations to six populations of poor colonizers from the
same phylum (Figure 2). Bacterial single-copy core genes estimated that genomes in
295 both subgroups were highly complete with a slight increase in average genome
completion of poor colonizers (93.7%) compared to good colonizers (90.1%). Despite the
higher estimated genome completion for populations of poor colonizers, estimated
metabolic module completion values were slightly yet significantly lower in this group
(Wilcoxon rank sum test with continuity correction, $V=958$, $p=5e-09$) (Figure 2,
300 Supplementary Table 7). Thus, these modules were systematically missing genes in
populations of poor colonizers, indicating their functionality was likely reduced, if not
absent.

These observations suggest that the ability to synthesize cellular building blocks,
cofactors and vitamins required for cellular maintenance and growth provides a
305 substantial advantage during secondary succession, highlighting that the competitive
advantages conferred by metabolic autonomy may outweigh the additional costs under
certain conditions. For the remainder of our study, we use the term 'high metabolic
independence' (HMI) to describe genomic evidence for a population's ability to synthesize

essential compounds, and ‘low metabolic independence’ (LMI) to describe the absence of, or reduction in, such capacity.

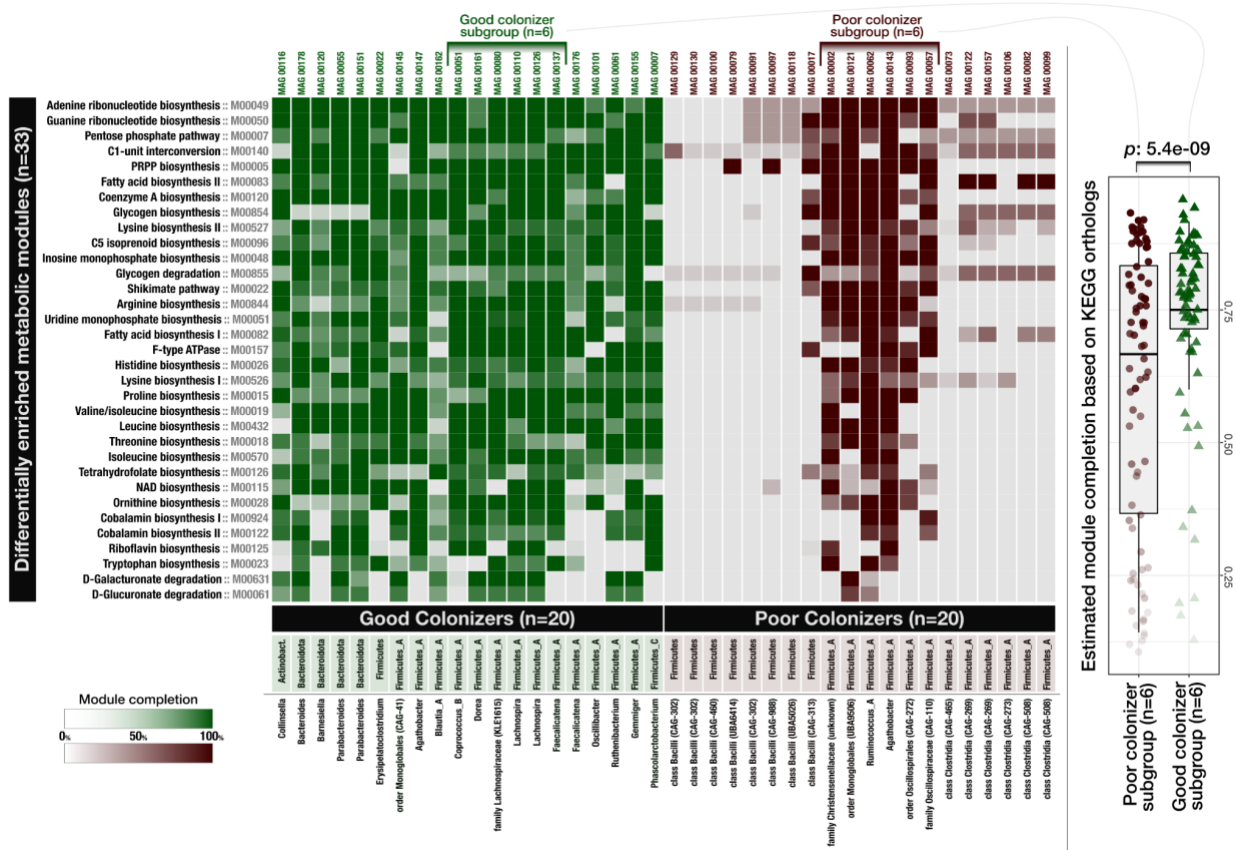


Figure 2. Distribution of metabolic modules across genomes of good and poor colonizers. Each data point in this heat map shows the level of completion of a given metabolic module (rows) in a given genome (columns). The box-plot on the right-side compares a subset of poor colonizer and good colonizer genomes, where each data point represents the level of completion of a given metabolic module in a genome and shows a statistically significant difference between the overall completion of metabolic modules between these subgroups (Wilcoxon rank sum test, $p=5.4e-09$). A high-resolution version of this figure is also available at <https://doi.org/10.6084/m9.figshare.15138720>.

While gut microbial ecosystems of healthy individuals include
320 microbes with both low- and high-metabolic independence, IBD
primarily selects for microbes with high-metabolic independence

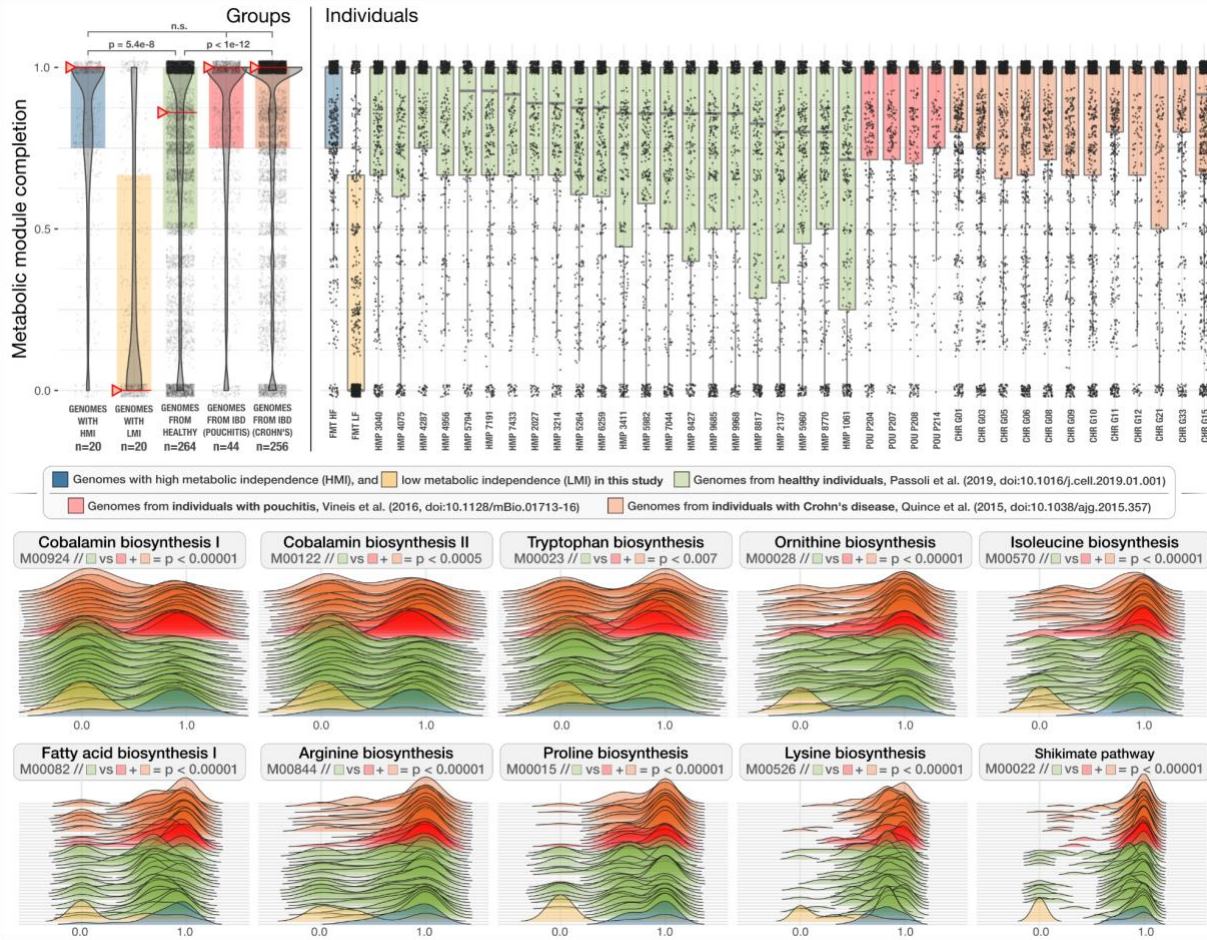
Our results so far show that while the healthy donor environment could support both HMI
and LMI populations (Figure 1, Supplementary Table 3), challenging microbes to colonize
a new environment or to withstand ecosystem perturbation during FMT selects for HMI
325 populations (Figure 2, Supplementary Table 7), suggesting that metabolic independence
is a more critical determinant of fitness during stress than during homeostasis. Based on
these observations, it is conceivable to hypothesize that (1) a gut environment in
homeostasis will support a large variety of microbial populations with a wide spectrum of
metabolic independence, and (2) a gut environment under stress will select for
330 populations with high metabolic independence, potentially leading to an overall reduction
in diversity.

To test these hypotheses, we compared genomes reconstructed from a cohort of healthy
individuals (Pasolli et al. 2019) to genomes reconstructed from individuals who were
diagnosed with inflammatory bowel disease (IBD). Our IBD dataset was composed of two
335 cohorts: a set of patients with pouchitis (Vineis et al. 2016), a form of IBD with similar
pathology to ulcerative colitis (De Preter et al. 2009), and a set of pediatric Crohn's
disease patients (Quince et al. 2015). The number of genomes per individual and the
average level of genome completeness per group were similar between healthy
individuals and those with IBD: overall, our analysis compared 264 genomes from 22
340 healthy individuals with an average completion of 90.4%, 44 genomes from 4 pouchitis
patients with an average completion of 89.2% and 256 genomes from 12 Crohn's disease
patients with an average completion of 94.1% (Supplementary Table 8). Intriguingly,
similar to the size differences between genomes of HMI populations and LMI populations
(2.8 Mbp versus 1.6 Mbp on average), genomes of microbial populations associated with
345 IBD patients were larger compared to those of microbial populations in healthy people
and averaged to 3.0 Mbp versus 2.6 Mbp, respectively (Supplementary Table 8). This
suggests that the environmental filters created by FMT and gastrointestinal inflammation

both select for microbial populations with larger genomes and potentially higher metabolic independence.

350 Next, we asked whether the completion of metabolic modules associated with colonization success and resilience during FMT differed between the genomes reconstructed from healthy and IBD individuals. The completion of the 33 metabolic modules was almost identical between the HMI populations revealed by FMT and microbial populations in IBD patients (Wilcoxon rank sum test, $p=0.5$) (Figure 3, 355 Supplementary Table 8). In contrast, the completion of these metabolic modules was significantly reduced in microbial populations in healthy individuals (Wilcoxon rank sum test, $p < 1e-07$) (Figure 3, Supplementary Table 8). Metabolic modules with the largest differences in completion between genomes from healthy and IBD individuals included biosynthesis of cobalamin, arginine, ornithine, tryptophan, isoleucine as well as the 360 Shikimate pathway (Figure 3, Supplementary Table 8), a seven step metabolic route bacteria use for the biosynthesis of aromatic amino acids (phenylalanine, tyrosine, and tryptophan) (Herrmann and Weaver 1999).

Our findings show that the same set of biosynthetic metabolic modules that distinguish good and poor colonizers during FMT were also differentially associated with populations 365 of IBD patients and healthy individuals. In particular, while healthy individuals harbored microbes with a broad spectrum of metabolic capacity, microbes from individuals who suffer from two different forms of IBD had significantly higher biosynthetic independence. It is conceivable that a stable gut microbial ecosystem is more likely to support LMI populations through metabolic cross-feeding, where vitamins, amino acids, and 370 nucleotides are exchanged between microbes (D'Souza et al. 2018). In contrast, host-mediated environmental stress in IBD likely disrupts such interactions and creates an ecological filter that selects for metabolic independence, which subsequently leads to loss of diversity and the dominance of organisms with large genomes that are often not as abundant or as competitive in states of homeostasis.



375

380

385

Figure 3. Distribution of metabolic modules in genomes reconstructed from healthy individuals and individuals with IBD. The boxplots in the top panels show the metabolic module completion values for (1) high- and (2) low-metabolic independence donor genomes identified in this study (blue and yellow), (3) genomes from healthy individuals (green), and (4) genomes from individuals with pouchitis (red) and Crohn's disease (orange). Each dot in a given boxplot represents one of 33 metabolic modules that were enriched in HMI FMT donor populations and the y-axis indicates its estimated completion. The leftmost top panel represents group averages and red whiskers indicate the median. The rightmost top panel shows the distribution of metabolic modules for individuals within each group. In the bottom panel the completion values for 10 of the 33 pathways are demonstrated as ridge-line plots. Each plot represents a single metabolic module where each layer corresponds to an individual, and the shape of the layer represents the completion of a given metabolic module across all genomes reconstructed from that individual. A high-resolution version of this figure is also available at <https://doi.org/10.6084/m9.figshare.15138720>.

390

These observations have implications for our understanding of the hallmarks of healthy gut microbial ecosystems. Defining the 'healthy gut microbiome' has been a major goal of human gut microbiome research (Bäckhed et al. 2012), which still remains elusive (Eisenstein 2020). Despite comprehensive investigations that considered core microbial

395 taxa (Arumugam et al. 2011; Lloyd-Price, Abu-Ali, and Huttenhower 2016) or guilds of
microbes that represent coherent functional groups (Wu et al. 2021), the search for
'biomarkers' of healthy gut microbiomes is ongoing (McBurney et al. 2019). Our findings
indicate that beyond the taxonomic diversity of a microbial community, a broad range of
metabolic independence represents a defining feature of a healthy gut microbiome.
Conversely, our findings also suggest that an enrichment of metabolically independent
populations could serve as an indicator of environmental stress in the human gut.
Detection of these metabolic markers is not influenced by fluctuations in taxonomic
composition or diversity, and represents a quantifiable feature of microbial communities
400 through genome-resolved metagenomic surveys.

Our findings offer a new, taxonomy-independent perspective on the determinants of
microbial resilience in the human gut environment under stress. Yet, our study is limited
to well-known metabolic pathways, which, given the extent of the unknown coding space
in microbial genomes (Vanni et al. 2020), are likely far from complete. Thus, the
405 enrichment of biosynthetic modules in HMI populations suggests that the ability to
synthesize essential biological compounds is necessary but likely insufficient to survive
environmental stress in the gut. Nevertheless, the finding that the same metabolic
modules that promote colonization success after FMT are also the hallmarks of resilience
in IBD suggests the presence of unifying ecological principles that govern microbial
410 diversity in distinct modes of stress, which warrants deeper investigation. Research into
the development of microbial therapeutics to reinstate homeostasis is continuously
intensifying (Jimenez et al., 2019) and the benefits of such treatments will critically
depend on successful engraftment of individual populations. Thus, considering their
degree of metabolic independence may prove crucial.

415 Conclusions

Our study identifies high metabolic independence conferred by the biosynthetic capacity
for amino acids, nucleotides, and essential micronutrients as a distinguishing hallmark of
microbial populations that colonize recipients of FMT and that thrive in IBD patients.
These findings highlight the functional complexity of the human gut microbiome whose

420 various interactions with the host are shaped through a network of microbial interactions
such as cross-feeding of macro- and micro-nutrients. Our study offers a simple model that
posits the following: microbial populations that are metabolically independent and those
that lack the means to synthesize essential metabolites co-occur in a healthy gut
environment in harmony, where their differential resilience to stress is indiscernible by
425 their taxonomy or relative abundance. However, the challenges associated with the
transfer to a new gut environment through FMT, or with host-mediated stress through
IBD, initiate an ecological filter that selects for microbes that can self-sustain in the
absence of ecosystem services associated with states of homeostasis. This model
provides a hypothesis that explains the dominance of low-abundance members of healthy
430 gut environments under stressful conditions, without any necessary direct causal
association with disease state. If the association between particular microbial taxa and
disease is solely driven by their superior metabolic independence, microbial therapies
that aim to treat complex diseases by adding microbes associated with healthy individuals
will be unlikely to compete with the adaptive processes that regulate complex gut
435 microbial ecosystems.

Materials and Methods

Sample collection and storage. We used a subset of individuals who participated in a
randomized clinical trial (Kao et al. 2017) and conducted a longitudinal FMT study of two
human cohorts (DA and DB), each consisting of one FMT donor and 5 FMT recipients of
440 that donor's stool. All recipients received vancomycin for a minimum of 10 days pre-FMT
at a dose of 125 mg four times daily. Three DA and two DB recipients received FMT via
pill, and two DA and three DB recipients received FMT via colonoscopy. All recipients had
recurrent *C. difficile* infection before FMT, and two DA recipients and one DB recipient
were also diagnosed with ulcerative colitis (UC). 24 stool samples were collected from
445 the DA donor over a period of 636 days, and 15 stool samples were collected from the
DB donor over a period of 532 days. Between 5 and 9 stool samples were collected from
each recipient over periods of 187 to 404 days, with at least one sample collected pre-
FMT and 4 samples collected post-FMT. This gave us a total of 109 stool samples from

all donors and recipients. Samples were stored at -80°C. (Supplementary Figure 1,
450 Supplementary Table 1)

Metagenomic short-read sequencing. We extracted the genomic DNA from frozen samples according to the centrifugation protocol outlined in MoBio PowerSoil kit with the following modifications: cell lysis was performed using a GenoGrinder to physically lyse the samples in the MoBio Bead Plates and Solution (5–10 min). After final precipitation,
455 the DNA samples were resuspended in TE buffer and stored at -20 °C until further analysis. Sample DNA concentrations were determined by PicoGreen assay. DNA was sheared to ~400 bp using the Covaris S2 acoustic platform and libraries were constructed using the Nugen Ovation Ultralow kit. The products were visualized on an Agilent Tapestation 4200 and size-selected using BluePippin (Sage Biosciences). The final
460 library pool was quantified with the Kapa Biosystems qPCR protocol and sequenced on the Illumina NextSeq500 in a 2 × 150 paired-end sequencing run using dedicated read indexing.

‘Omics workflows. Whenever applicable, we automated and scaled our ‘omics analyses using the bioinformatics workflows implemented by the program `anvi-run-workflow`
465 (Shaiber et al. 2020) in anvi’o 7.1 (Eren et al. 2015, 2021). Anvi’o workflows implement numerous steps of bioinformatics tasks including short-read quality filtering, assembly, gene calling, functional annotation, hidden Markov model search, metagenomic read-recruitment, metagenomic binning, and phylogenomics. Workflows use Snakemake (Köster and Rahmann 2012) and a tutorial is available at the URL
470 <http://merenlab.org/anvio-workflows/>. The following sections detail these steps.

Taxonomic composition of metagenomes based on short reads. We used Kraken2 v2.0.8-beta (Wood, Lu, and Langmead 2019) with the NCBI’s RefSeq bacterial, archaeal, viral and viral neighbors genome databases to calculate the taxonomic composition within short-read metagenomes.

475 **Assembly of metagenomic short reads.** To minimize the impact of random sequencing errors in our downstream analyses, we used the program `iu-filter-quality-minoche` to process short metagenomic reads, which is implemented in illumina-utils v2.11 (Eren et al. 2013) and removes low-quality reads according to the criteria outlined by Minoche et

al. (Minoche, Dohm, and Himmelbauer 2011). IDBA_UD v1.1.2 (Peng et al. 2012)
480 assembled quality-filtered short reads into longer contiguous sequences (contigs),
although we needed to recompile IDBA_UD with a modified header file so it could process
150bp paired-end reads.

Processing of contigs. We use the following strategies to process both sequences we
obtained from our assemblies and those we obtained from reference genomes. Briefly,
485 we used (1) `anvi-gen-contigs-database` on contigs to compute k-mer frequencies and
identify open reading frames (ORFs) using Prodigal v2.6.3 (Hyatt et al. 2010), (2) `anvi-
run-hmms` to identify sets of bacterial (Campbell et al. 2013) and archaeal (Rinke et al.
2013) single-copy core genes using HMMER v3.2.1 (Eddy 2011), (3) `anvi-run-ncbi-cogs`
to annotate ORFs with functions from the NCBI's Clusters of Orthologous Groups (COGs)
490 (Tatusov et al. 2003), and (4) `anvi-run-kegg-kofams` to annotate ORFs with functions
from the KOfam HMM database of KEGG orthologs (KOs) (Aramaki et al. 2020; M.
Kanehisa and Goto 2000). To predict the approximate number of genomes in
metagenomic assemblies we used the program `anvi-display-contigs-stats`, which
calculates the mode of the frequency of single-copy core genes as described previously
495 (Delmont and Eren 2016).

**Metagenomic read recruitment, reconstructing genomes from metagenomes,
determination of genome taxonomy and ANI.** We recruited metagenomic short reads
to contigs using Bowtie2 v2.3.5 (Langmead and Salzberg 2012) and converted resulting
SAM files to BAM files using samtools v1.9 (Li et al. 2009). We profiled the resulting BAM
500 files using the program `anvi-profile` with the flag `--min-contig-length` set to 2500 to
eliminate shorter sequences to minimize noise. We then used the program `anvi-merge`
to combine all read recruitment profiles into a single anvi'o merged profile database for
downstream visualization, binning, and statistical analyses (the DOI
10.6084/m9.figshare.14331236 gives access to reproducible data objects). We then used
505 `anvi-cluster-contigs` to group contigs into 100 initial bins using CONCOCT v1.1.0
(Alneberg et al. 2014), `anvi-refine` to manually curate initial bins with conflation error
based on tetranucleotide frequency and differential coverage signal across all samples,
and `anvi-summarize` to report final summary statistics for each gene, contig, and bin.

We used the program `anvi-rename-bins` to identify bins that were more than 70%
510 complete and less than 10% redundant and store them in a new collection as
metagenome-assembled genomes (MAGs), discarding lower quality bins from
downstream analyses. GTBD-tk v0.3.2 (Chaumeil et al. 2019) assigned taxonomy to each
of our MAGs using GTDB r89 (Parks et al. 2018), but to assign species- and subspecies-
level taxonomy for `DA_MAG_00057`, `DA_MAG_00011`, `DA_MAG_00052` and
515 `DA_MAG_00018`, we used `anvi-get-sequences-for-hmm-hits` to recover DNA
sequences for bacterial single-copy core genes that encode ribosomal proteins, and
searched them in the NCBI's nucleotide collection (nt) database using BLAST (Altschul
et al. 1990). Finally, the program `anvi-compute-genome-similarity` calculated pairwise
genomic average nucleotide identity (gANI) of our genomes using PyANI v0.2.9 (Pritchard
520 et al. 2016).

Criteria for MAG detection in metagenomes. Using mean coverage to assess the
occurrence of populations in a given sample based on metagenomic read recruitment can
yield misleading insights, since this strategy cannot accurately distinguish reference
sequences that represent very low-abundance environmental populations from those
525 sequences that do not represent an environmental population in a sample yet still recruit
reads from non-target populations due to the presence of conserved genomic regions.
Thus, we relied upon the 'detection' metric, which is a measure of the proportion of the
nucleotides in a given sequence that are covered by at least one short read. We
considered a population to be detected in a metagenome if anvi'o reported a detection
530 value of at least 0.25 for its genome (whether it was a metagenome-assembled or isolate
genome). Values of detection in metagenomic read recruitment results often follow a
bimodal distribution for populations that are present and absent (see Supplementary
Figure 2 in ref. (Utter et al. 2020)), thus 0.25 is an appropriate cutoff to eliminate false-
positive signal in read recruitment results for populations that are absent.

535 **Identification of MAGs that represent multiple subpopulations.** To identify
subpopulations of MAGs in metagenomes, we used the anvi'o command `anvi-gen-
variability-profile` with the `--quince-mode` flag which exported single-nucleotide variant
(SNV) information for all MAGs after read recruitment. We then used DESMAN v2.1.1

(Quince et al. 2017) to analyze SNVs to determine the number and distribution of subpopulations represented by a single genome. To account for non-specific mapping that can inflate the number of estimated subpopulations, we removed any subpopulation that made up less than 1% of the entire population explained by a single MAG. To account for noise due to low coverage, we only investigated subpopulations for MAGs for which the mean non-outlier coverage of single-copy core genes was at least 10X.

Criteria for colonization of a recipient by a MAG for colonization dynamics analyses (Supplementary Information). We applied the set of criteria described in Supplementary Figure 4 to determine whether or not a MAG successfully colonized a recipient, and to confidently assign colonization or non-colonization phenotypes to each MAG/recipient pair where the MAG was detected in the donor sample used for transplant into the recipient. If these criteria were met, we then determined whether the MAG was detected in any post-FMT recipient sample taken more than 7 days after transplant. If not, the MAG/recipient pair was considered a non-colonization event. If the MAG was detected in the recipient greater than 7 days post-FMT, we used subpopulation information to determine if any subpopulation present in the donor and absent in the recipient pre-FMT was detected in the recipient more than 7 days post-FMT. If this was the case, we considered this to represent a colonization event. See Supplementary Figure 4 for a complete outline of all possible cases.

Phylogenomic tree construction. To concatenate and align amino acid sequences of 46 single-copy core (Campbell et al. 2013) ribosomal proteins that were present in all of our *Bifidobacterium* MAGs and reference genomes, we ran the `anvi'o` command ``anvi-get-sequences-for-hmm-hits`` with the ``--return-best-hit``, ``--get-aa-sequence`` and ``--concatenate`` flags, and the ``--align-with`` flag set to ``muscle`` to use MUSCLE v3.8.1551 (Edgar 2004) for alignment. We then ran ``anvi-gen-phylogenomic-tree`` with default parameters to compute a phylogenomic tree using FastTree 2.1 (Price, Dehal, and Arkin 2010).

Analysis of metabolic modules and enrichment. We calculated the level of completeness for a given KEGG module (Minoru Kanehisa et al. 2014, 2017) in our genomes using the program ``anvi-estimate-metabolism``, which leveraged previous

annotation of genes with KEGG orthologs (KOs) (see the section 'Processing of contigs').
570 Then, the program `anvi-compute-functional-enrichment` determined whether a given
metabolic module was enriched in a group of genomes based on the output from the
program `anvi-estimate-metabolism`. The URL [https://anvio.org/help/7.1/programs/anvi-
575 estimate-metabolism/](https://anvio.org/help/7.1/programs/anvi-estimate-metabolism/) serves a tutorial for this program which details the modes of usage
and output file formats. The statistical approach for enrichment analysis is defined
elsewhere (Shaiber et al. 2020), but briefly it computes enrichment scores for functions
(or metabolic modules) within groups by fitting a binomial generalized linear model (GLM)
to the occurrence of each function or complete metabolic module in each group, and then
computing a Rao test statistic, uncorrected p-values, and corrected q-values. We
580 considered any function or metabolic module with a q-value less than 0.05 to be 'enriched'
in its associated group if it was also at least 75% complete and present in at least 50% of
the group members.

**Determination of MAGs representing good and poor colonizers for metabolic
enrichment analysis.** We classified MAGs as good colonizers if, in all 5 recipients, they
were detected in the donor sample used for transplantation as well as the recipient more
585 than 7 days post-FMT. We classified MAGs as poor colonizers as those that, in at least
3 recipients, were detected in the donor sample used for FMT but were not detected in
the recipient at least 7 days post-FMT. We reduced the number of good colonizer MAGs
to be the same as the number of poor colonizer MAGs for metabolic enrichment analysis
by selecting only those populations that were the most prevalent in the Canadian gut
590 metagenomes.

Ordination plots. We used the R vegan v2.4-2 package `metaMDS` function to perform
nonmetric multidimensional scaling (NMDS) with Horn-Morisita dissimilarity distance to
compare taxonomic composition between donor, recipient, and global metagenomes. We
visualized ordination plots using R ggplot2.

595 Code and Data Availability

Raw sequencing data for donor and recipient metagenomes are stored under the NCBI BioProject [PRJNA701961](#) (see Supplementary Table 1 for accession numbers for each sample). The URL <https://merenlab.org/data/fmt-gut-colonization> serves a reproducible bioinformatics workflow and gives access to ad hoc scripts, usage instructions, and
600 intermediate data objects to reproduce findings in our study. Supplementary tables are accessible also via doi:[10.6084/m9.figshare.14138405](https://doi.org/10.6084/m9.figshare.14138405).

Acknowledgements

We thank Mitchell L. Sogin, Eugene B. Chang, Samuel H. Light, and Howard A. Shuman for helpful discussions, Ryan Moore and Ozcan C. Esen for technical support, and Nicola
605 Segata and the members of the Segata group for their assistance with genomes from healthy gut metagenomes. We also thank Kaiyu Wu, Robyn Louie and Linda Ward of the IPC Research Laboratory at the University of Calgary for their help with patient recruitment and sampling. This project was supported by the GI Research Foundation (GIRF) and the Mutchnik Family Fund. Additionally, ARW acknowledges support from the
610 Robert C. and Mary Jane Gallo Scholarship Fund; JF acknowledges support from the Alissa and Gianna Carlino Fellowship in Celiac Disease Research; BJ acknowledges support from the Cancer Center Support grant P30CA014599 and Digestive Diseases Research Core Center P30 DK42086; and IV acknowledges support from the National Science Foundation Graduate Research Fellowship (1746045).

615 Author Contributions

AME, TL, BJ conceived the study. JZD, MS, DK, TL recruited patients, performed transplantation experiments, and collected samples. ARW, JF, AME performed primary data analyses. IV developed research tools. KL, STML, HGM performed sample processing and sequencing. FT, AS, EF, JMR, CQ, MKY, AY contributed to data analyses

620 and interpretation. DTR, BJ, TL, and AME directed research. ARW, JF, AME wrote the paper with critical input from all authors.

Competing Interests

Authors declare no competing financial interests.

References

- 625 Almeida, Cátia, Rita Oliveira, Raquel Soares, and Pedro Barata. 2020. "Influence of Gut Microbiota Dysbiosis on Brain Function: A Systematic Review." *Porto Biomedical Journal* 5 (2). <https://doi.org/10.1097/j.pbj.0000000000000059>.
- Alneberg, Johannes, Brynjar Smári Bjarnason, Ino de Bruijn, Melanie Schirmer, Joshua Quick, Umer Z. Ijaz, Leo Lahti, Nicholas J. Loman, Anders F. Andersson, and
630 Christopher Quince. 2014. "Binning Metagenomic Contigs by Coverage and Composition." *Nature Methods* 11 (11): 1144–46.
- Altschul, S. F., W. Gish, W. Miller, E. W. Myers, and D. J. Lipman. 1990. "Basic Local Alignment Search Tool." *Journal of Molecular Biology* 215 (3): 403–10.
- Aramaki, Takuya, Romain Blanc-Mathieu, Hisashi Endo, Koichi Ohkubo, Minoru
635 Kanehisa, Susumu Goto, and Hiroyuki Ogata. 2020. "KofamKOALA: KEGG Ortholog Assignment Based on Profile HMM and Adaptive Score Threshold." *Bioinformatics* 36 (7): 2251–52.
- Arumugam, Manimozhayan, Jeroen Raes, Eric Pelletier, Denis Le Paslier, Takuji Yamada, Daniel R. Mende, Gabriel R. Fernandes, et al. 2011. "Enterotypes of the
640 Human Gut Microbiome." *Nature* 473 (7346): 174–80.
- Bäckhed, Fredrik, Claire M. Fraser, Yehuda Ringel, Mary Ellen Sanders, R. Balfour Sartor, Philip M. Sherman, James Versalovic, Vincent Young, and B. Brett Finlay. 2012. "Defining a Healthy Human Gut Microbiome: Current Concepts, Future Directions, and Clinical Applications." *Cell Host & Microbe* 12 (5): 611–22.
- 645 Baumgart, Daniel C., and Simon R. Carding. 2007. "Inflammatory Bowel Disease: Cause and Immunobiology." *The Lancet* 369 (9573): 1627–40.
- Biesalski, Hans K. 2016. "Nutrition Meets the Microbiome: Micronutrients and the Microbiota." *Annals of the New York Academy of Sciences* 1372 (1): 53–64.
- Bowers, Robert M., Nikos C. Kyrpides, Ramunas Stepanauskas, Miranda Harmon-Smith, Devin Doud, T. B. K. Reddy, Frederik Schulz, et al. 2017. "Minimum
650 Information about a Single Amplified Genome (MISAG) and a Metagenome-Assembled Genome (MIMAG) of Bacteria and Archaea." *Nature Biotechnology* 35 (8): 725–31.
- Campbell, James H., Patrick O'Donoghue, Alisha G. Campbell, Patrick Schwientek,
655 Alexander Sczyrba, Tanja Woyke, Dieter Söll, and Mircea Podar. 2013. "UGA Is an Additional Glycine Codon in Uncultured SR1 Bacteria from the Human Microbiota."

Proceedings of the National Academy of Sciences of the United States of America
110 (14): 5540–45.

- 660 Chaumeil, Pierre-Alain, Aaron J. Mussig, Philip Hugenholtz, and Donovan H. Parks.
2019. “GTDB-Tk: A Toolkit to Classify Genomes with the Genome Taxonomy
Database.” *Bioinformatics*, November.
<https://doi.org/10.1093/bioinformatics/btz848>.
- 665 Chen, Lin-Xing, Karthik Anantharaman, Alon Shaiber, A. Murat Eren, and Jillian F.
Banfield. 2020. “Accurate and Complete Genomes from Metagenomes.” *Genome
Research* 30 (3): 315–33.
- Chow, Janet, Haiqing Tang, and Sarkis K. Mazmanian. 2011. “Pathobionts of the
Gastrointestinal Microbiota and Inflammatory Disease.” *Current Opinion in
Immunology* 23 (4): 473–80.
- 670 Clooney, Adam G., Julia Eckenberger, Emilio Laserna-Mendieta, Kathryn A. Sexton,
Matthew T. Bernstein, Kathy Vagianos, Michael Sargent, et al. 2021. “Ranking
Microbiome Variance in Inflammatory Bowel Disease: A Large Longitudinal
Intercontinental Study.” *Gut* 70 (3): 499–510.
- 675 Costello, Elizabeth K., Keaton Stagaman, Les Dethlefsen, Brendan J. M. Bohannon,
and David A. Relman. 2012. “The Application of Ecological Theory toward an
Understanding of the Human Microbiome.” *Science* 336 (6086): 1255–62.
- David, Lawrence A., Arne C. Materna, Jonathan Friedman, Maria I. Campos-Baptista,
Matthew C. Blackburn, Allison Perrotta, Susan E. Erdman, and Eric J. Alm. 2014.
“Host Lifestyle Affects Human Microbiota on Daily Timescales.” *Genome Biology* 15
(7): R89.
- 680 Delmont, Tom O., and A. Murat Eren. 2016. “Identifying Contamination with Advanced
Visualization and Analysis Practices: Metagenomic Approaches for Eukaryotic
Genome Assemblies.” *PeerJ* 4 (March): e1839.
- 685 Delmont, Tom O., Christopher Quince, Alon Shaiber, Özcan C. Esen, Sonny Tm Lee,
Michael S. Rappé, Sandra L. McLellan, Sebastian Lücker, and A. Murat Eren.
2018. “Nitrogen-Fixing Populations of Planctomycetes and Proteobacteria Are
Abundant in Surface Ocean Metagenomes.” *Nature Microbiology* 3 (7): 804–13.
- De Preter, Vicky, Veerle Bulteel, Peter Suenart, Karen Paula Geboes, Gert De
Hertogh, Anja Luybaerts, Karel Geboes, Kristin Verbeke, and Paul Rutgeerts. 2009.
“Pouchitis, Similar to Active Ulcerative Colitis, Is Associated with Impaired Butyrate
690 Oxidation by Intestinal Mucosa.” *Inflammatory Bowel Diseases* 15 (3): 335–40.
- Donaldson, Gregory P., S. Melanie Lee, and Sarkis K. Mazmanian. 2016. “Gut
Biogeography of the Bacterial Microbiota.” *Nature Reviews. Microbiology* 14 (1):
20–32.
- 695 D’Souza, Glen, Shraddha Shitut, Daniel Preussger, Ghada Yousif, Silvio Waschina, and
Christian Kost. 2018. “Ecology and Evolution of Metabolic Cross-Feeding
Interactions in Bacteria.” *Natural Product Reports* 35 (5): 455–88.
- Durack, Juliana, and Susan V. Lynch. 2019. “The Gut Microbiome: Relationships with
Disease and Opportunities for Therapy.” *The Journal of Experimental Medicine* 216
(1): 20–40.
- 700 Eddy, Sean R. 2011. “Accelerated Profile HMM Searches.” *PLoS Computational
Biology* 7 (10): e1002195.
- Edgar, Robert C. 2004. “MUSCLE: Multiple Sequence Alignment with High Accuracy

- and High Throughput." *Nucleic Acids Research* 32 (5): 1792–97.
- 705 Eiseman, B., W. Silen, G. S. Bascom, and A. J. Kauvar. 1958. "Fecal Enema as an Adjunct in the Treatment of Pseudomembranous Enterocolitis." *Surgery* 44 (5): 854–59.
- Eisenstein, Michael. 2020. "The Hunt for a Healthy Microbiome." *Nature* 577 (7792): S6–8.
- 710 Eren, A. Murat, Özcan C. Esen, Christopher Quince, Joseph H. Vineis, Hilary G. Morrison, Mitchell L. Sogin, and Tom O. Delmont. 2015. "Anvi'o: An Advanced Analysis and Visualization Platform for 'Omics Data." *PeerJ* 3 (October): e1319.
- Eren, A. Murat, Evan Kiefl, Alon Shaiber, Iva Veseli, Samuel E. Miller, Matthew S. Schechter, Isaac Fink, et al. 2021. "Community-Led, Integrated, Reproducible Multi-Omics with Anvi'o." *Nature Microbiology* 6 (1): 3–6.
- 715 Eren, A. Murat, Joseph H. Vineis, Hilary G. Morrison, and Mitchell L. Sogin. 2013. "A Filtering Method to Generate High Quality Short Reads Using Illumina Paired-End Technology." *PloS One* 8 (6): e66643.
- Feng, Lihui, Arjun S. Raman, Matthew C. Hibberd, Jiye Cheng, Nicholas W. Griffin, Yangqing Peng, Semen A. Leyn, Dmitry A. Rodionov, Andrei L. Osterman, and Jeffrey I. Gordon. 2020. "Identifying Determinants of Bacterial Fitness in a Model of Human Gut Microbial Succession." *Proceedings of the National Academy of Sciences of the United States of America* 117 (5): 2622–33.
- 720 Grehan, Martin J., Thomas Julius Borody, Sharyn M. Leis, Jordana Campbell, Hazel Mitchell, and Antony Wettstein. 2010. "Durable Alteration of the Colonic Microbiota by the Administration of Donor Fecal Flora." *Journal of Clinical Gastroenterology* 44 (8): 551–61.
- Herrmann, Klaus M., and Lisa M. Weaver. 1999. "THE SHIKIMATE PATHWAY." *Annual Review of Plant Physiology and Plant Molecular Biology* 50 (June): 473–503.
- 730 Human Microbiome Project Consortium. 2012. "Structure, Function and Diversity of the Healthy Human Microbiome." *Nature* 486 (7402): 207–14.
- Hyatt, Doug, Gwo-Liang Chen, Philip F. Locascio, Miriam L. Land, Frank W. Larimer, and Loren J. Hauser. 2010. "Prodigal: Prokaryotic Gene Recognition and Translation Initiation Site Identification." *BMC Bioinformatics* 11 (March): 119.
- 735 Isaac, Sandrine, Jose U. Scher, Ana Djukovic, Nuria Jiménez, Dan R. Littman, Steven B. Abramson, Eric G. Pamer, and Carles Ubeda. 2017. "Short- and Long-Term Effects of Oral Vancomycin on the Human Intestinal Microbiota." *The Journal of Antimicrobial Chemotherapy* 72 (1): 128–36.
- Jimenez, Miguel, Robert Langer, and Giovanni Traverso. 2019. "Microbial Therapeutics: New Opportunities for Drug Delivery." *The Journal of Experimental Medicine* 216 (5): 1005–9.
- 740 Joossens, Marie, Geert Huys, Margo Cnockaert, Vicky De Preter, Kristin Verbeke, Paul Rutgeerts, Peter Vandamme, and Severine Vermeire. 2011. "Dysbiosis of the Faecal Microbiota in Patients with Crohn's Disease and Their Unaffected Relatives." *Gut* 60 (5): 631–37.
- 745 Kanehisa, M., and S. Goto. 2000. "KEGG: Kyoto Encyclopedia of Genes and Genomes." *Nucleic Acids Research* 28 (1): 27–30.
- Kanehisa, Minoru, Miho Furumichi, Mao Tanabe, Yoko Sato, and Kanae Morishima. 2017. "KEGG: New Perspectives on Genomes, Pathways, Diseases and Drugs."

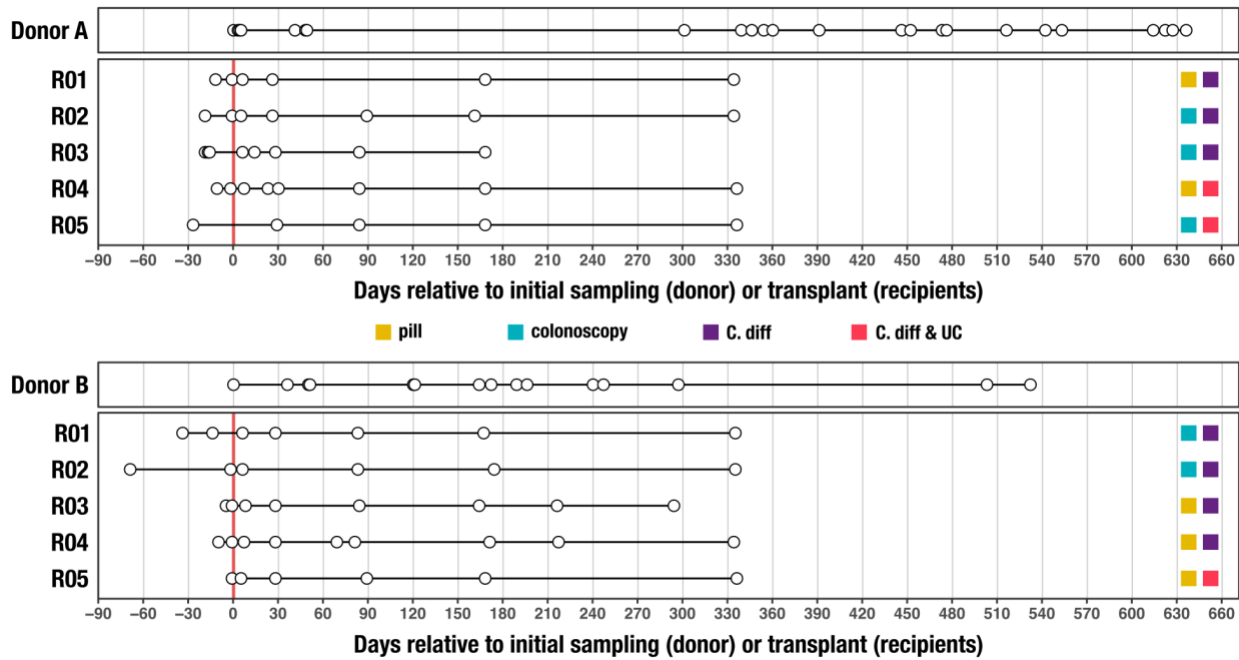
- Nucleic Acids Research* 45 (D1): D353–61.
- 750 Kanehisa, Minoru, Susumu Goto, Yoko Sato, Masayuki Kawashima, Miho Furumichi, and Mao Tanabe. 2014. “Data, Information, Knowledge and Principle: Back to Metabolism in KEGG.” *Nucleic Acids Research* 42 (Database issue): D199–205.
- Kao, Dina, Brandi Roach, Marisela Silva, Paul Beck, Kevin Rioux, Gilaad G. Kaplan, Hsiu-Ju Chang, et al. 2017. “Effect of Oral Capsule- vs Colonoscopy-Delivered
- 755 Fecal Microbiota Transplantation on Recurrent Clostridium Difficile Infection: A Randomized Clinical Trial.” *JAMA: The Journal of the American Medical Association* 318 (20): 1985–93.
- Khoruts, Alexander, Johan Dicksved, Janet K. Jansson, and Michael J. Sadowsky. 2010. “Changes in the Composition of the Human Fecal Microbiome after
- 760 Bacteriotherapy for Recurrent Clostridium Difficile-Associated Diarrhea.” *Journal of Clinical Gastroenterology* 44 (5): 354–60.
- Koenig, Jeremy E., Aymé Spor, Nicholas Scalfone, Ashwana D. Fricker, Jesse Stombaugh, Rob Knight, Lergus T. Angenent, and Ruth E. Ley. 2011. “Succession of Microbial Consortia in the Developing Infant Gut Microbiome.” *Proceedings of the National Academy of Sciences of the United States of America* 108 Suppl 1 (March): 4578–85.
- 765 Koropatkin, Nicole M., Elizabeth A. Cameron, and Eric C. Martens. 2012. “How Glycan Metabolism Shapes the Human Gut Microbiota.” *Nature Reviews. Microbiology* 10 (5): 323–35.
- 770 Köster, Johannes, and Sven Rahmann. 2012. “Snakemake—a Scalable Bioinformatics Workflow Engine.” *Bioinformatics* 28 (19): 2520–22.
- Langmead, Ben, and Steven L. Salzberg. 2012. “Fast Gapped-Read Alignment with Bowtie 2.” *Nature Methods* 9 (4): 357–59.
- 775 Lee, Sonny T. M., Stacy A. Kahn, Tom O. Delmont, Alon Shaiber, Özcan C. Esen, Nathaniel A. Hubert, Hilary G. Morrison, Dionysios A. Antonopoulos, David T. Rubin, and A. Murat Eren. 2017. “Tracking Microbial Colonization in Fecal Microbiota Transplantation Experiments via Genome-Resolved Metagenomics.” *Microbiome* 5 (1): 50.
- 780 Li, Heng, Bob Handsaker, Alec Wysoker, Tim Fennell, Jue Ruan, Nils Homer, Gabor Marth, Goncalo Abecasis, Richard Durbin, and 1000 Genome Project Data Processing Subgroup. 2009. “The Sequence Alignment/Map Format and SAMtools.” *Bioinformatics* 25 (16): 2078–79.
- Lloyd-Price, Jason, Galeb Abu-Ali, and Curtis Huttenhower. 2016. “The Healthy Human Microbiome.” *Genome Medicine* 8 (1): 51.
- 785 Lloyd-Price, Jason, Cesar Arze, Ashwin N. Ananthakrishnan, Melanie Schirmer, Julian Avila-Pacheco, Tiffany W. Poon, Elizabeth Andrews, et al. 2019. “Multi-Omics of the Gut Microbial Ecosystem in Inflammatory Bowel Diseases.” *Nature* 569 (7758): 655–62.
- 790 Lynch, Susan V., and Oluf Pedersen. 2016. “The Human Intestinal Microbiome in Health and Disease.” *The New England Journal of Medicine* 375 (24): 2369–79.
- Martens, Eric C., Herbert C. Chiang, and Jeffrey I. Gordon. 2008. “Mucosal Glycan Foraging Enhances Fitness and Transmission of a Saccharolytic Human Gut Bacterial Symbiont.” *Cell Host & Microbe* 4 (5): 447–57.
- Martens, J. H., H. Barg, M. J. Warren, and D. Jahn. 2002. “Microbial Production of

- 795 Vitamin B12.” *Applied Microbiology and Biotechnology* 58 (3): 275–85.
- McBurney, Michael I., Cindy Davis, Claire M. Fraser, Barbara O. Schneeman, Curtis Huttenhower, Kristin Verbeke, Jens Walter, and Marie E. Latulippe. 2019. “Establishing What Constitutes a Healthy Human Gut Microbiome: State of the Science, Regulatory Considerations, and Future Directions.” *The Journal of Nutrition* 149 (11): 1882–95.
- 800 Messer, J. S., E. R. Liechty, O. A. Vogel, and E. B. Chang. 2017. “Evolutionary and Ecological Forces That Shape the Bacterial Communities of the Human Gut.” *Mucosal Immunology* 10 (3): 567–79.
- Minoche, André E., Juliane C. Dohm, and Heinz Himmelbauer. 2011. “Evaluation of Genomic High-Throughput Sequencing Data Generated on Illumina HiSeq and Genome Analyzer Systems.” *Genome Biology* 12 (11): R112.
- 805 Nood, Els van, Anne Vrieze, Max Nieuwdorp, Susana Fuentes, Erwin G. Zoetendal, Willem M. de Vos, Caroline E. Visser, et al. 2013. “Duodenal Infusion of Donor Feces for Recurrent *Clostridium Difficile*.” *The New England Journal of Medicine* 368 (5): 407–15.
- 810 Ott, S. J., M. Musfeldt, D. F. Wenderoth, J. Hampe, O. Brant, U. R. Fölsch, K. N. Timmis, and S. Schreiber. 2004. “Reduction in Diversity of the Colonic Mucosa Associated Bacterial Microflora in Patients with Active Inflammatory Bowel Disease.” *Gut* 53 (5): 685–93.
- 815 Parks, Donovan H., Maria Chuvoshina, David W. Waite, Christian Rinke, Adam Skarszewski, Pierre-Alain Chaumeil, and Philip Hugenholtz. 2018. “A Standardized Bacterial Taxonomy Based on Genome Phylogeny Substantially Revises the Tree of Life.” *Nature Biotechnology* 36 (10): 996–1004.
- Pasoli, Edoardo, Francesco Asnicar, Serena Manara, Moreno Zolfo, Nicolai Karcher, Federica Armanini, Francesco Beghini, et al. 2019. “Extensive Unexplored Human Microbiome Diversity Revealed by Over 150,000 Genomes from Metagenomes Spanning Age, Geography, and Lifestyle.” *Cell* 176 (3): 649–62.e20.
- 820 Peng, Yu, Henry C. M. Leung, S. M. Yiu, and Francis Y. L. Chin. 2012. “IDBA-UD: A de Novo Assembler for Single-Cell and Metagenomic Sequencing Data with Highly Uneven Depth.” *Bioinformatics* 28 (11): 1420–28.
- 825 Plichta, Damian R., Daniel B. Graham, Sathish Subramanian, and Ramnik J. Xavier. 2019. “Therapeutic Opportunities in Inflammatory Bowel Disease: Mechanistic Dissection of Host-Microbiome Relationships.” *Cell* 178 (5): 1041–56.
- Price, Morgan N., Paramvir S. Dehal, and Adam P. Arkin. 2010. “FastTree 2-- Approximately Maximum-Likelihood Trees for Large Alignments.” *PLoS One* 5 (3): e9490.
- 830 Pritchard, Leighton, Rachel H. Glover, Sonia Humphris, John G. Elphinstone, and Ian K. Toth. 2016. “Genomics and Taxonomy in Diagnostics for Food Security: Soft-Rotting Enterobacterial Plant Pathogens.” *Analytical Methods* 8 (1): 12–24.
- 835 Quince, Christopher, Tom O. Delmont, Sébastien Raguideau, Johannes Alneberg, Aaron E. Darling, Gavin Collins, and A. Murat Eren. 2017. “DESMAN: A New Tool for de Novo Extraction of Strains from Metagenomes.” *Genome Biology* 18 (1): 181.
- Quince, Christopher, Umer Zeeshan Ijaz, Nick Loman, A. Murat Eren, Delphine Saulnier, Julie Russell, Sarah J. Haig, et al. 2015. “Extensive Modulation of the Fecal Metagenome in Children with Crohn’s Disease During Exclusive Enteral
- 840

- Nutrition.” *The American Journal of Gastroenterology* 110 (12): 1718–29; quiz 1730.
- Rinke, Christian, Patrick Schwientek, Alexander Sczyrba, Natalia N. Ivanova, Iain J. Anderson, Jan-Fang Cheng, Aaron Darling, et al. 2013. “Insights into the
845 Phylogeny and Coding Potential of Microbial Dark Matter.” *Nature* 499 (7459): 431–37.
- Rothschild, Daphna, Omer Weissbrod, Elad Barkan, Alexander Kurilshikov, Tal Korem, David Zeevi, Paul I. Costea, et al. 2018. “Environment Dominates over Host Genetics in Shaping Human Gut Microbiota.” *Nature* 555 (7695): 210–15.
- 850 Schirmer, Melanie, Ashley Garner, Hera Vlamakis, and Ramnik J. Xavier. 2019. “Microbial Genes and Pathways in Inflammatory Bowel Disease.” *Nature Reviews. Microbiology* 17 (8): 497–511.
- Schmidt, Thomas S. B., Jeroen Raes, and Peer Bork. 2018. “The Human Gut Microbiome: From Association to Modulation.” *Cell* 172 (6): 1198–1215.
- 855 Shahinas, Dea, Michael Silverman, Taylor Sittler, Charles Chiu, Peter Kim, Emma Allen-Vercoe, Scott Weese, Andrew Wong, Donald E. Low, and Dylan R. Pillai. 2012. “Toward an Understanding of Changes in Diversity Associated with Fecal Microbiome Transplantation Based on 16S rRNA Gene Deep Sequencing.” *mBio* 3 (5): e00338–12.
- 860 Shaiber, Alon, Amy D. Willis, Tom O. Delmont, Simon Roux, Lin-Xing Chen, Abigail C. Schmid, Mahmoud Yousef, et al. 2020. “Functional and Genetic Markers of Niche Partitioning among Enigmatic Members of the Human Oral Microbiome.” *Genome Biology* 21 (1): 292.
- 865 Sharon, Itai, Michael J. Morowitz, Brian C. Thomas, Elizabeth K. Costello, David A. Relman, and Jillian F. Banfield. 2013. “Time Series Community Genomics Analysis Reveals Rapid Shifts in Bacterial Species, Strains, and Phage during Infant Gut Colonization.” *Genome Research* 23 (1): 111–20.
- Sheth, Ravi U., Mingqiang Li, Weiqian Jiang, Peter A. Sims, Kam W. Leong, and Harris H. Wang. 2019. “Spatial Metagenomic Characterization of Microbial Biogeography
870 in the Gut.” *Nature Biotechnology* 37 (8): 877–83.
- Smillie, Christopher S., Jenny Sauk, Dirk Gevers, Jonathan Friedman, Jaeyun Sung, Ilan Youngster, Elizabeth L. Hohmann, et al. 2018. “Strain Tracking Reveals the Determinants of Bacterial Engraftment in the Human Gut Following Fecal Microbiota Transplantation.” *Cell Host & Microbe* 23 (2): 229–40.e5.
- 875 Sokol, Harry, and Philippe Seksik. 2010. “The Intestinal Microbiota in Inflammatory Bowel Diseases: Time to Connect with the Host.” *Current Opinion in Gastroenterology* 26 (4): 327–31.
- Stewart, Christopher J., Nadim J. Ajami, Jacqueline L. O’Brien, Diane S. Hutchinson, Daniel P. Smith, Matthew C. Wong, Matthew C. Ross, et al. 2018. “Temporal
880 Development of the Gut Microbiome in Early Childhood from the TEDDY Study.” *Nature* 562 (7728): 583–88.
- Swidsinski, Alexander, Jutta Weber, Vera Loening-Baucke, Laura P. Hale, and Herbert Lochs. 2005. “Spatial Organization and Composition of the Mucosal Flora in Patients with Inflammatory Bowel Disease.” *Journal of Clinical Microbiology* 43 (7):
885 3380–89.
- Tatusov, Roman L., Natalie D. Fedorova, John D. Jackson, Aviva R. Jacobs, Boris

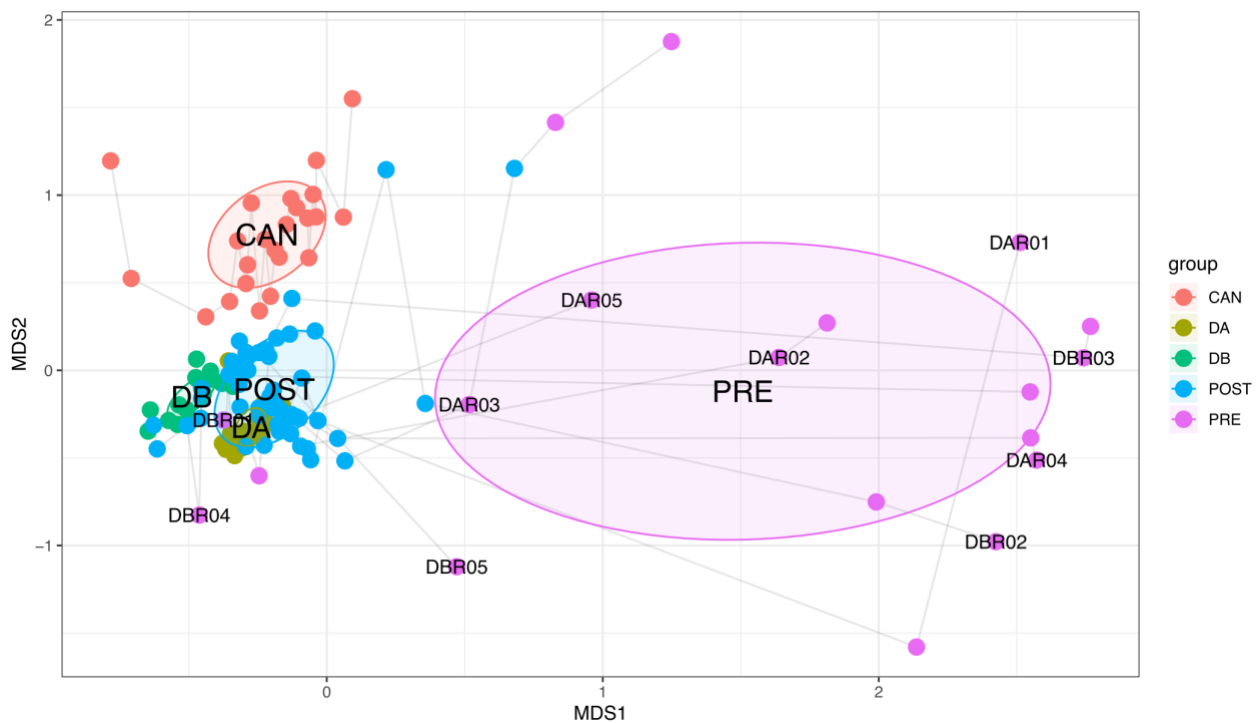
- Kiryutin, Eugene V. Koonin, Dmitri M. Krylov, et al. 2003. "The COG Database: An Updated Version Includes Eukaryotes." *BMC Bioinformatics* 4 (September): 41.
- 890 Utter, Daniel R., Gary G. Borisy, A. Murat Eren, Colleen M. Cavanaugh, and Jessica L. Mark Welch. 2020. "Metapangenomics of the Oral Microbiome Provides Insights into Habitat Adaptation and Cultivar Diversity." *Genome Biology* 21 (1): 293.
- Vanni, Chiara, Matthew S. Schechter, Silvia G. Acinas, Albert Barberán, Pier Luigi Buttigieg, Emilio O. Casamayor, Tom O. Delmont, et al. 2020. "Unifying the Global Coding Sequence Space Enables the Study of Genes with Unknown Function across Biomes." *Cold Spring Harbor Laboratory*.
895 <https://doi.org/10.1101/2020.06.30.180448>.
- Vineis, Joseph H., Daina L. Ringus, Hilary G. Morrison, Tom O. Delmont, Sushila Dalal, Laura H. Raffals, Dionysios A. Antonopoulos, et al. 2016. "Patient-Specific *Bacteroides* Genome Variants in Pouchitis." *mBio* 7 (6): e01713–16,
900 [/mbio/7/6/e01713–16.atom](https://doi.org/10.1128/mBio.01713-16).
- Walter, Jens, Anissa M. Armet, B. Brett Finlay, and Fergus Shanahan. 2020. "Establishing or Exaggerating Causality for the Gut Microbiome: Lessons from Human Microbiota-Associated Rodents." *Cell* 180 (2): 221–32.
- 905 Wexler, Aaron G., and Andrew L. Goodman. 2017. "An Insider's Perspective: *Bacteroides* as a Window into the Microbiome." *Nature Microbiology*.
<https://doi.org/10.1038/nmicrobiol.2017.26>.
- Wood, Derrick E., Jennifer Lu, and Ben Langmead. 2019. "Improved Metagenomic Analysis with Kraken 2." *Genome Biology* 20 (1): 257.
- 910 Wu, Guojun, Naisi Zhao, Chenhong Zhang, Yan Y. Lam, and Liping Zhao. 2021. "Guild-Based Analysis for Understanding Gut Microbiome in Human Health and Diseases." *Genome Medicine* 13 (1): 22.
- Yasuda, Koji, Keunyoung Oh, Boyu Ren, Timothy L. Tickle, Eric A. Franzosa, Lynn M. Wachtman, Andrew D. Miller, et al. 2015. "Biogeography of the Intestinal Mucosal and Lumenal Microbiome in the Rhesus Macaque." *Cell Host & Microbe* 17 (3):
915 385–91.
- Zmora, Niv, Jotham Suez, and Eran Elinav. 2019. "You Are What You Eat: Diet, Health and the Gut Microbiota." *Nature Reviews. Gastroenterology & Hepatology* 16 (1): 35–56.

Supplementary Figures



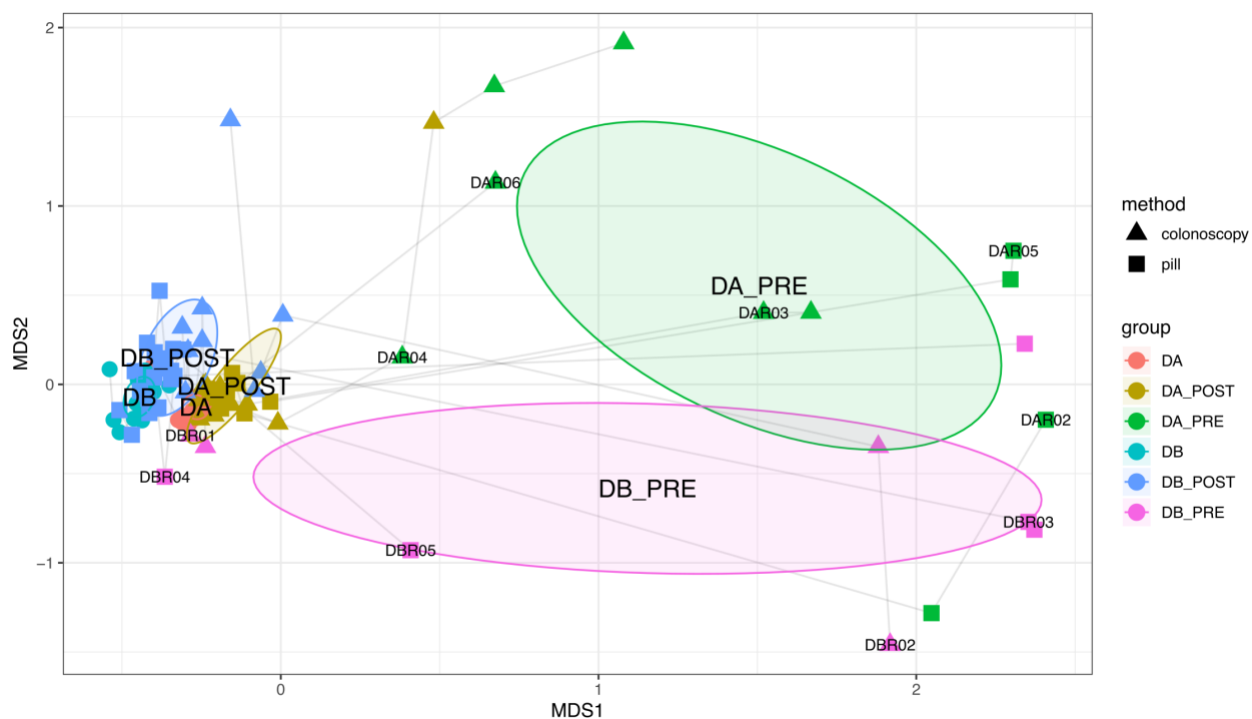
920

Supplementary Figure 1. Timeline of stool samples collected from FMT study. Each circle represents a stool sample collected from either an FMT donor or FMT recipient. The thicker, red vertical line at day 0 represents the FMT event for each recipient. FMT method (pill or colonoscopy) and FMT recipient health and disease state (C. diff - chronic recurrent *Clostridium difficile* infection, UC - ulcerative colitis) are indicated on the right.



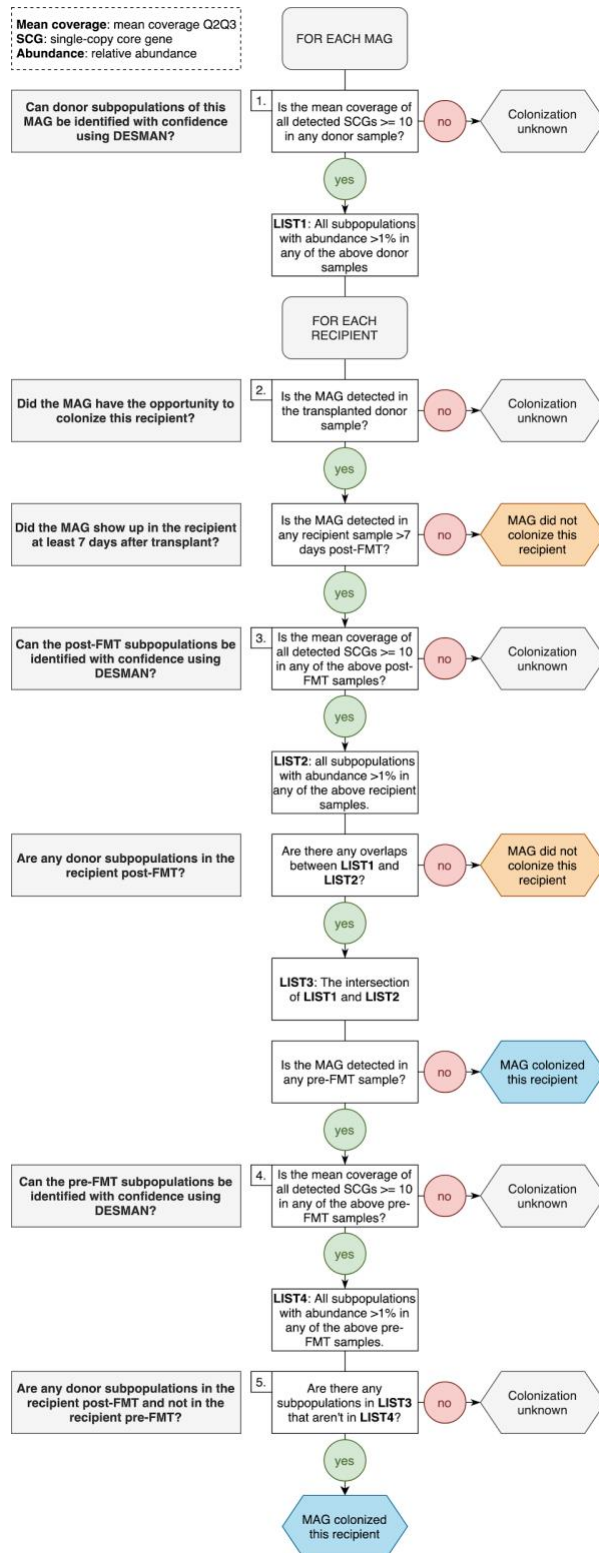
925

Supplementary Figure 2. Nonmetric multidimensional scaling (NMDS) ordination of the taxonomic composition of donor, recipient, and Canadian gut metagenomes at the genus level based on Morisita-Horn dissimilarity. Samples from the same participant are joined by lines with the earliest time point labeled. CAN: Canadian gut metagenomes, DA: donor A, DB: donor B, POST: recipients post-FMT, PRE: recipients pre-FMT.



Supplementary Figure 3. Nonmetric multidimensional scaling (NMDS) ordination of the taxonomic composition of the donor and recipient metagenomes at genus level based on Morisita-Horn dissimilarity. Samples from the same participant are joined by lines with the earliest time point labeled. DA_POST: donor A recipients post-FMT, DA_PRE: donor A recipients pre-FMT, DA: donor A, DB_POST: donor B recipients post-FMT, DB_PRE: donor B recipients pre-FMT, DB: donor B.

935



Supplementary Figure 4. A flowchart outlining our method to assign successful colonization, failed colonization, or undetermined colonization phenotypes to donor-derived populations in the recipients of that donor's stool.

Supplementary Tables ()

940 **Supplementary Table 1: Description of FMT study and stool samples collected.** a) Description of FMT donor stool samples and SRA accession numbers. b) Description of FMT recipient samples and SRA accession numbers. c) Description of transplantation events.

945 **Supplementary Table 2: Description of FMT metagenomes and co-assemblies.** a) Metagenome SRA accession numbers and numbers of metagenomic short-reads sequenced and mapped to co-assemblies and MAGs. b) Phylum level taxonomic composition of metagenomes. c) Genus level taxonomic composition of metagenomes. d) Summary statistics for contigs from metagenome co-assemblies.

950 **Supplementary Table 3: Description of MAGs.** a) Summary statistics and taxonomic assignments for MAGs. b) and c) Detection of Donor A and Donor B MAGs in FMT metagenomes, respectively. d) and e) Detection of Donor A and Donor B MAGs in global gut metagenomes, respectively. f) and g) Detection summary statistics of Donor A and Donor B MAGs in global gut metagenomes, respectively. h) and i) Mean non-outlier coverage of Donor A and Donor B MAG single-copy core genes in FMT metagenomes.

Supplementary Table 4: Accession numbers of gut metagenomes from 17 countries.

955 **Supplementary Table 5: MAG subpopulation information.** a) and b) Number of Donor A and Donor B MAG subpopulations detected in FMT metagenomes, respectively. c) and d) Subpopulation composition of Donor A and Donor B MAGs in FMT metagenomes, respectively.

Supplementary Table 6: MAG/recipient pair colonization outcomes and MAG mean coverage in the 2nd and 3rd quartiles in stool samples used for transplantation.

960 **Supplementary Table 7: Description of HMI vs. LMI populations.** a) Taxonomic assignments and genome size estimates for high- and low-metabolic independence populations. b) KEGG module completeness information for high- and low-metabolic independence populations. c) Raw KEGG module enrichment information for high- and low-metabolic independence populations. d) KEGG module enrichment and categorical information for the 33 modules enriched in high-metabolic independence populations. e) and f) Completeness information for the 33 modules enriched in high-metabolic independence populations in all high- and low-metabolic independence populations.

965 **Supplementary Table 8:** a) List of genomes from healthy individuals and individuals with IBD. b) Module completion values across genomes.